Delta-toxin production deficiency in *Staphylococcus aureus*: a diagnostic marker of bone and joint infection chronicity linked with osteoblast invasion and biofilm formation

F. Valour[1,2,3,4], J.-P. Rasigade[2,3,4], S. Trouillet-Assant[3], J. Gagnaire[2], A. Bouaziz[1], J. Karsenty[1], C. Lacour[2], M. Bes[2,3], S. Lustig[3,4,5], T. Bénet[6], C. Chidiac[1,3,4], J. Etienne[2,3,4], F. Vandenesch[2,3,4], T. Ferry[1,3,4] and F. Laurent[2,3,4], on behalf of the Lyon BJI Study Group

1) *Department of Infectious Diseases,* 2) *Department of Microbiology, French National Reference Centre for Staphylococci, Hospices Civils de Lyon,* 3) *INSERM U1111, International Centre for Infectiology Research,* 4) *Claude Bernard Lyon 1 University,* 5) *Orthopaedic Surgery department and* 6) *Department of Infection Control and Epidemiology, Hospices Civils de Lyon, Edouard Herriot Hospital, Lyon, France*

Abstract

Biofilm formation, intra-osteoblastic persistence, small-colony variants (SCVs) and the dysregulation of *agr*, the major virulence regulon, are possibly involved in staphylococcal bone and joint infection (BJI) pathogenesis. We aimed to investigate the contributions of these mechanisms among a collection of 95 *Staphylococcus aureus* clinical isolates from 64 acute (67.4%) and 31 chronic (32.6%) first episodes of BJI. The included isolates were compared for internalization rate, cell damage and SCV intracellular emergence using an *ex vivo* model of human osteoblast infection. Biofilm formation was assessed in a microbead immobilization assay (BioFilm Ring test). Virulence gene profiles were assessed by DNA microarray. Seventeen different clonal complexes were identified among the screened collection. The staphylococcal internalization rate in osteoblasts was significantly higher for chronic than acute BJI isolates, regardless of the genetic background. Conversely, no differences regarding cytotoxicity, SCV emergence, biofilm formation and virulence gene distribution were observed. Additionally, *agr* dysfunction, detected by the lack of delta-toxin production using whole-cell matrix-assisted laser desorption ionization time-of-flight (MALDI-TOF) analysis (n = 15; 15.8%), was significantly associated with BJI chronicity, osteoblast invasion and biofilm formation. These findings provide new insights into MSSA BJI pathogenesis, suggesting the correlation between chronicity and staphylococcal osteoblast invasion. This adaptive mechanism, along with biofilm formation, is associated with *agr* dysfunction, which can be routinely assessed by delta-toxin detection using MALDI-TOF spectrum analysis, possibly providing clinicians with a diagnostic marker of BJI chronicity at the time of diagnosis.

Keywords: Biofilm formation, bone and joint infection, delta-toxin, matrix-assisted laser desorption ionization time-of-flight mass spectrometry, osteoblast invasion, *Staphylococcus aureus*

Original Submission: 29 June 2014; **Revised Submission:** 21 January 2015; **Accepted:** 24 January 2015

Editor: J.L. Mainardi

Article published online: 10 February 2015

Corresponding author: F. Valour; Hospices Civils de Lyon, Groupement Hospitalier Nord, Laboratoire de Bactériologie; 103 Grande Rue de la Croix-Rousse, 69004 Lyon, France

E-mail: florent.valour@chu-lyon.fr

Introduction

Staphylococcus aureus is the leading cause of bone and joint infections (BJI), described as difficult-to-treat clinical entities due to frequent bacterial persistence leading to chronicity and relapse, despite 3–6-month antibiotic therapy associated with complex surgical procedures [1,2]. The management strongly differs between acute BJI, for which debridement with implant

http://dx.doi.org/10.1016/j.cmi.2015.01.026

retention is recommended, and chronic forms, which require the removal of any orthopaedic implants [3]. Patients with chronic BJI are arbitrarily defined, without any reliable biological indicator, as patients with active BJI for over a month.

As BJI evolution delay can directly impact the medical and surgical management of patients, an objective bacterial marker of BJI chronicity is actually sorely lacking. Based on fundamental studies, three staphylococcal phenotypic virulence factors are thought to be potentially associated with BJI chronicity. First, *S. aureus* is highly capable of forming biofilm—a surface-attached heterogeneous bacterial community encased with a self-produced matrix composed of proteins, polysaccharides and DNA. Due to its role as physical, chemical and enzymatic barrier, biofilm formation has been shown to be a mechanism for evading host defences and resisting the effect of antimicrobials, contributing to relapsing/chronic infections [4,5]. Then, if *S. aureus* is primarily an extracellular pathogen, it has been reported to invade and persist in non-professional phagocytic host cells, including osteoblasts, leading to the constitution of a bacterial reservoir responsible for recurrence [6–8]. Finally, intracellular lifestyle and growth within biofilm are accompanied by significant changes in gene and protein expression, as well as metabolic activity, leading to bacterial phenotype switching to small-colony variants (SCVs), a particular population of persisting bacteria which has been associated with BJI persistence [9–11]. In addition to these phenotypic virulence mechanisms, the dysregulation of accessory gene regulator (*agr*), a major regulon controlling the expression of a plethora of *S. aureus* virulence factors, has been associated with persistent infections [12–14].

In this context, we aimed to assess these different phenotypic and molecular bacterial markers for clinical relevance toward early identification of BJI chronicity at the time of diagnosis.

Materials and methods

Ethical statements

This study received the approval of the French South-East ethics committee (reference number 2013-018).

BJI definitions

All methicillin-susceptible *S. aureus* (MSSA) isolates responsible for a first episode of BJI in our institution from 2001 to 2011 were considered for inclusion. Patients with diabetic foot-related or decubitus ulcer-related BJI were excluded because of the particular pathophysiology and management of these infections. Corresponding clinical data were retrospectively collected from medical records on a standardized case record form, and included demographic characteristics and patient co-morbidities (summarized in the modified Charlson co-morbidity index), BJI clinical presentation, presence of biological inflammatory syndrome (i.e. C-reactive protein plasma level $\geq$10 mg/L and/or white blood cell count $\geq$10 000/mm^3), and outcome. BJI were defined as acute (infection lasting for $\leq$4 weeks) or chronic infections. Treatment failure included persistent infection under appropriate antimicrobial therapy, including the need for new surgery >5 days after the first one, and relapse after antimicrobial discontinuation.

Evaluation of staphylococcal interaction with human osteoblasts

Staphylococcal interaction with osteoblasts was assessed in a gentamicin protection assay, as previously described [15–17]. All cell culture reagents were obtained from Gibco (Paisley, UK).

MG63 osteoblastic cell culture. The human osteoblastic cell line MG63 (CRL-1427), purchased from LGC Standards (Teddington, UK), was cultured in Dulbecco's modified Eagle's medium supplemented with 10% fetal calf serum, 25 mM HEPES, 2 mM L-glutamine, 100 U/mL penicillin, and 100 mg/L streptomycin. Before the assays, the osteoblasts were seeded at 40 000 cells per well into 24-well tissue culture plates (Falcon, Le Pont de Claix, France) in 1 mL of growth medium and were cultured for 2 days until 70–80% confluence.

Bacterial suspension standardization and infection. Overnight staphylococcal culture suspensions were diluted five-fold in fresh brain–hearth infusion broth and further incubated in a gyratory shaker for 3 h at 37°C to obtain mid-exponential-phase cultures. These suspensions were washed, sonicated to minimize clumping, and resuspended in antibiotic-free medium at a concentration corresponding to an MOI of 100, using the following previously established regression formula correlating bacterial density (CFU/mL) with optical density at 600 nm (OD_{600}): CFU/mL = ($7 \times 10_8 \times OD_{600}$) – ($3 \times 10_7$) (data not shown). The normalized bacterial suspensions were then added to osteoblast cultures. After 2 h of co-culture, the infected osteoblasts were incubated for 1 h with growth medium supplemented with 200 mg/L gentamicin (PAA, Pasching, Austria) to kill the remaining extracellular staphylococcal cells. After 1 h, the cell culture medium was replaced by growth medium supplemented with 40 µg/mL gentamicin for 24 h to kill bacteria released upon host cell lysis, so preventing these bacteria from infecting new host cells.

Evaluation of staphylococcal-induced cytotoxicity. After 24 h, lactate dehydrogenase (LDH) release from damaged cells was quantified in the cell culture supernatant using a colorimetric method with a Dimension Vista automated clinical chemistry analyser (Siemens Healthcare Diagnostics, Tarryton, NY). The per cent mortality of osteoblasts was assessed by comparing LDH release into the infected cell supernatant to that of uninfected cells that were either left intact (lower control) or fully

lysed by osmotic shock (higher control) and was calculated as follows: ((LDH infected cells – LDH lower control)/(LDH higher control – LDH lower control)) × 100. LDH release was expressed relative to the 8325-4 reference strain.

Quantification of internalized bacteria. After 24 h of gentamicin treatment, aliquots of infected osteoblasts were lysed by a 10-min incubation period in sterile water. Suspension dilutions of these lysates were spiral-plated using a WASP automated plater (AES Chemunex, Bruz, France). Colonies were enumerated using an EasyCount automated plate reader (AES Chemunex). Intracellular bacterial counts were expressed relative to the 8325-4 reference strain.

Evaluation of SCV phenotype switching. A commonly used operational definition of SCVs based on colony size states that colonies with a size less than one-fifth of that of the wild-type strain can be considered as SCVs [11]. Previous reports were based on visual inspection of cultures by an operator. To eliminate operator dependency, SCV quantification was performed using an automated process in which a high-resolution picture of each plate was taken and analysed by means of the image analysis software ImageJ (ImageJ, Rasband, W.S., National Institutes of Health, Bethesda, MD, USA, 1997–2012) [18], with a customized macro involving colour thresholding, watershed algorithm and particle analysis, to extract the distribution of colony areas. Wild-type colony area was defined as the median area of all colonies (because median is robust to outliers, the presence of SCVs did not influence this measure significantly) and SCVs were defined, according to the usual operational definition, as colonies with an area less than one-fifth of the median area.

Each isolate was evaluated in duplicate in a single experiment. The *S. aureus* 8325-4 laboratory strain, which has been well characterized with regard to its capacity to invade osteoblasts, was used as a control in each experiment [15,16].

Biofilm formation

The kinetics of biofilm formation was explored using the BioFilm Ring test (BioFilm Control, Saint Beauzire, France), as initially described by Chavant et al. [19]. Briefly, this technique is based on the immobilization of magnetic microbeads when embedded in bacterial biofilms. After adjusting the OD_{600} of overnight bacterial suspensions at 1 ± 0.05, the suspensions were diluted 1 : 250 in fresh brain–heart infusion medium, mixed with 1% of magnetic microbeads suspension ("tonner"), and deposited in triplicate in a 96-well microplate. Every 1 h for 5 h, the wells of one plate were covered with 100 µL of contrast solution (white opaque oil). The plate was then placed on a dedicated magnet support for 1 min for contact magnetization and was then scanned with a plate reader to obtain an image of the bottom of each well. During contact magnetization, free beads are attracted to the centre of the bottom of each well, forming a spot, whereas the beads captured within a biofilm remain in suspension. The BioFilm Control software (BioFilm Elements) analyses the images of each well before and after magnetization and calculates the BioFilm Index (BFI). Each observed BFI (BFI_o) was normalized as a proportion of the immobilized beads (so-called RBI for 'Relative Bead Immobilization') and was compared with controls with ($BFI_{reference}$) and without ($BFI_{minimal}$) beads using the following formula: $RBI = ((BFI_{reference} - BFI_o) / (BFI_{reference} - BFI_{minimal}))^{0.5}$ [19,20]. Forty isolates were tested, including all *agr*-deficient (i.e. delta-haemolysin-negative) isolates. Others were randomly selected among the most prevalent clonal complexes in a proportion representative of the repartition of the entire collection.

Accessory gene regulator functionality

The multifunctional regulatory RNAIII, the main effector of the *agr* system [21], is also a messenger RNA for the delta-toxin, whose production is consequently a surrogate marker of *agr* functionality [22]. Recently, it was shown that delta-toxin production, and hence *agr* function, can be assessed using whole cell matrix-assisted laser desorption ionization time-of-flight (MALDI-TOF) mass spectrometry (MS) during the routine MS-mediated microbiological identification process [23]. Consequently, *agr* functionality was assessed by the evaluation of delta-toxin production from whole bacterial cells by MALDI-TOF-MS spectrum analysis using an Axima Assurance® mass spectrometer (Shimadzu Biotech, Noisiel, France) piloted by LaunchPad® software (version 2.8.4.20081127, Shimadzu Biotech) with the conventional settings for bacterial identification [23,24]. Delta-toxin peak at 3005 ± 5 Thomson (or its allelic variant at 3015 ± 5 Th) was searched manually in the MS spectrum, as previously described [23].

Molecular characterization

DNA was extracted and purified using commercial extraction kits (DNeasy kit and QIAcube instrument; Qiagen, Hilden, Germany), according to the manufacturer's protocol. The DNA microarray Identibac *S. aureus* genotyping® (Alere Technologies, Jena, Germany) used in this study and the related procedures have been previously described in detail [25]. This microarray allows the detection of 332 different target sequences corresponding to 185 genes and their allelic variants. The isolate clonal complexes were determined by the comparison of the hybridization profiles to previously typed multilocus sequence typing reference strains [25].

Statistical analysis

Descriptive statistics were used to estimate the frequencies of the study variables, expressed as the means and 95% confidence

intervals (95% CIs). Non-parametric statistical methods were used throughout to compare the study groups (the chi-squared test with Yates' correction, if needed, the Mann–Whitney *U*-test for two-group difference analysis, and the Kruskal–Wallis test for multiple pairwise comparisons) and to investigate correlations (Spearman coefficient), as appropriate. Phenotypic factors (internalization, LDH release and SCV phenotype switching rates), delta-toxin expression and virulence genes were included in a binary logistic regression model to disclose risk factors for chronicity, including variables with *p*-values <0.15 in the univariate analysis in the final model. For all tests, a p-value <0.05 was taken as significant. All analyses were performed using SPSS software version 17.0 (SPSS, Chicago, IL, USA).

Results

Population characteristics

A total of 211 patients with MSSA BJI were identified; six were excluded because of the lack of available clinical data and three due to chronic osteomyelitis resulting from diabetic perforating ulcers. Among the 202 remaining patients, 86 isolates had not been stored in the laboratory. Nineteen isolates collected at the time of relapse and two stable SCVs were excluded. In total, 95 isolates responsible for 64 (67.4%) acute and 31 (32.6%) chronic BJI were included (Table 1).

MSSA from chronic BJI shows a higher capacity to invade human osteoblasts

The mean relative internalization rate within osteoblasts was significantly higher for chronic BJI isolates (240.7% of 8325-4 internalization rate; 95% CI, 171.3–310.2) than for acute BJI isolates (162.7%; 95% CI, 132.3–193.0; p 0.035) (Fig. 1a). Moreover, the internalization rate was correlated with the infection evolution delay, i.e. the time from symptom onset to microbiological diagnosis (Spearman coefficient 0.29; p 0.005) (Fig. 1b). No difference was observed between the two groups regarding cytotoxicity at 24 h, with 10.7% (95% CI, 8.3–13.1) and 7.6% (95% CI, 4.8–10.4) of cell death (p 0.152), respectively (Fig. 1c). LDH release was not correlated with BJI evolution delay (Spearman coefficient −0.07; p 0.512). Similarly, no difference in the capacities of the two groups to convert to the SCV phenotype was observed, with SCV proportions of 3.3% (95% CI, 2.8–3.7) and 3.4% (95% CI, 2.5–4.2) for the acute and chronic MSSA BJI isolates, respectively (p 1.000) (Fig. 1d).

Biofilm formation does not differ between acute and chronic MSSA BJI isolates

The total immobilization of magnetic beads, reflecting biofilm formation, was observed within 5 h for all isolates. The kinetics of biofilm formation was similar for the acute and chronic BJI isolates (Fig. 2). Of note, microarray data indicated that all isolates harboured the biofilm-associated genes *icaA*, *icaC* and *icaD* (see below).

Genetic background analysis reveals a high diversity among BJI MSSA clinical isolates, with no difference in virulence gene distribution in acute and chronic BJI isolates

Seventeen different clonal complexes were identified, of which seven included more than five isolates (Table 2). No significant difference regarding the distribution of these clonal complexes

TABLE 1. Characteristics of the 95 included patients with methicillin-susceptible *Staphylococcus aureus* bone and joint infection

	Total (*n* = 95)	Acute BJI (*n* = 64)	Chronic BJI (*n* = 31)	p-value
Demographic characteristics				
Sex (male)	60 (63%)	38 (59%)	22 (71%)	0.272
Age (year)	53.6 (49.6–57.6)	56.1 (51.3–60.8)	48.5 (49.6–57.6)	0.105
Modified CCI	2.6 (2.1–3.2)	2.9 (2.2–3.6)	2.0 (1.1–2.9)	0.148
BJI type				
Native septic arthritis	12 (13%)	10 (16%)	2 (7%)	0.351
Native osteomyelitis	12 (13%)	2 (3%)	10 (32%)	<0.001
Vertebral osteomyelitis	7 (7%)	5 (8%)	2 (7%)	0.856
Orthopaedic device infection	64 (67%)	47 (73%)	17 (55%)	0.070
Osteosynthesis	32 (50%)	23 (49%)	9 (53%)	0.777
Prosthetic joint	29 (45%)	22 (49%)	7 (41%)	0.689
Others	3 (5%)	2 (4%)	1 (6%)	0.691
Biological inflammatory syndrome	88 (93%)	59 (92%)	29 (94%)	0.811
CRP level (mg/L)	170.5 (141.7–199.3)	209.8 (174.4-245.3)	86.23 (52.7–119.8)	<0.0001
WBC (/mm^3)	10 790 (9985–11 600)	11 060 (10 140–11 970)	10 220 (8538–11 910)	0.098
Neutrophil count (/mm^3)	8129 (7338–8921)	8577 (7706–9448)	7169 (5492–8846)	0,009
Management				
Surgical treatment	83 (87%)	57 (89%)	26 (84%)	0.700
Antimicrobial treatment duration (weeks)	27.8 (23.5–32.0)	26.4 (21.2–31.7)	30.6 (22.8–38.4)	0.244
Outcome				
Treatment failure linked with the same strain	21 (22%)	14 (22%)	7 (23%)	0.938

Abbreviations: BJI, Bone and joint infection; CCI, Charlson comorbidity index; CRP, C-reactive protein; WBC, white blood cell.
Note: Results are presented as effective (%) and mean (95%CI) values. Comparisons between acute and chronic BJI were performed using a two-tailed Fisher's exact test or a Mann–Whitney *U*-test, as appropriate.

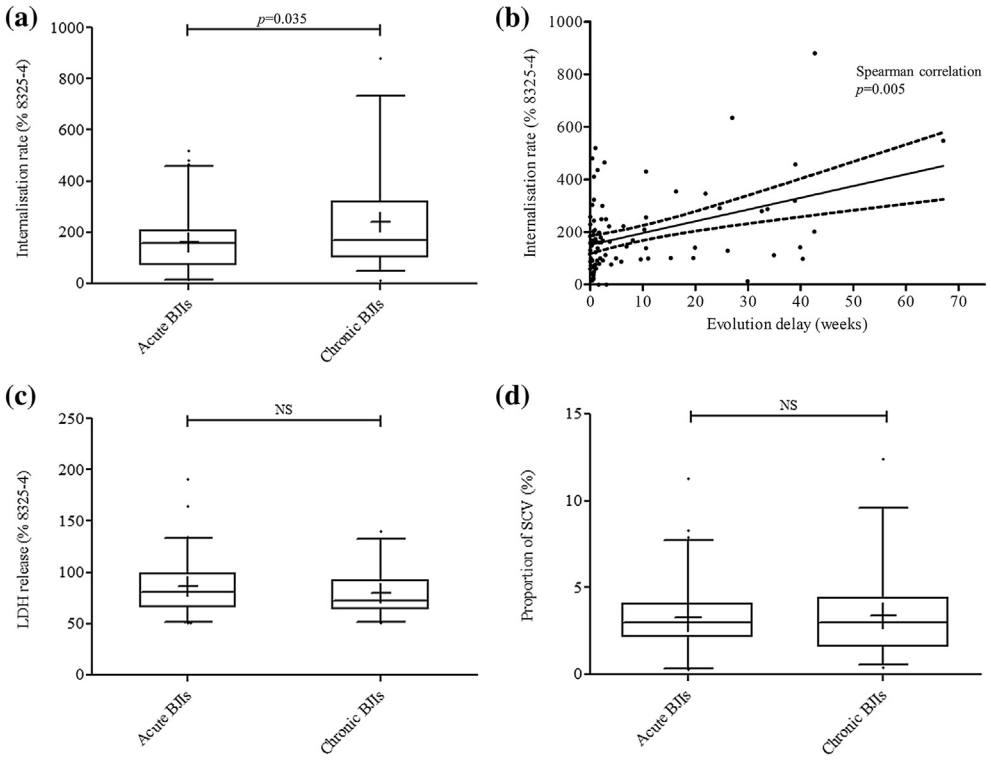

FIG. 1. Comparison of interactions between human osteoblasts and methicillin-susceptible *Staphylococcus aureus* (MSSA) isolates obtained from acute and chronic bone and joint infections (BJI). (a) Internalization rate of MSSA isolates within human osteoblasts; (b) Correlation between the internalization rate of MSSA clinical isolates and BJI evolution delay; (c) Cytotoxicity rate induced by human osteoblast infection by MSSA isolates; (d) proportion of phenotype switching to small-colony variants (SCVs).

between acute and chronic BJI was observed (p 0.408). Using multiple pairwise comparisons (Kruskal–Wallis test), no differences were identified between the different clusters with regard to their capacity to invade bone cells (p 0.446), cause cell damage (p = 0.368), switch SCV phenotypes (p 0.054), or form biofilm (p 0.347) (Table 2, Fig. 3).

The distribution of virulence genes of the 95 BJI MSSA isolates is presented in Table 3. No difference regarding the prevalence of these virulence factors between the acute and chronic BJI MSSA isolates was noted. Logistic regression failed to identify one of these virulence genes as a determinant for BJI chronicity (Table 3).

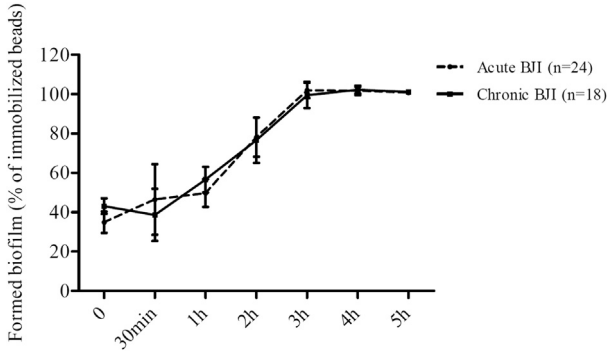

FIG. 2. Comparison of biofilm formation by methicillin-susceptible *Staphylococcus aureus* (MSSA) isolates obtained from acute and chronic bone and joint infections (BJI).

agr dysfunction, detected through the absence of delta-toxin production, is associated with MSSA BJI chronicity, osteoblast invasion and biofilm formation

Eighty isolates (84.2%) were considered to have a functional *agr* system, as a delta-toxin peak (n = 76) or its allelic variant (n = 4) was detected using MALDI-TOF-MS analysis. Interestingly, delta-toxin negative strains tended to be more represented among chronic (n = 8, 25.8%) than acute (n = 7, 10.9%) BJI isolates (p 0.062), and the evolution delay of BJI was significantly higher in the delta-toxin negative isolates (17.4 weeks; 95% CI, 6.1–28.8) than in those with a functional *agr* system (6.4 weeks; 95% CI, 4.0–8.9; p 0.045). Compared with delta-toxin positive isolates, the absence of delta-toxin expression was associated with a higher internalization rate (337.1% of the 8325-4 internalization rate (95% CI, 219.5–454.7) versus 160.2% (95% CI, 133.9–186.5); p < 0.001), lower osteoblast cytotoxicity (64.5% of 8325-4 LDH release (95% CI, 57.1–71.8) versus 87.3% (95%

TABLE 2. Distribution of the major methicillin-susceptible *Staphylococcus aureus* clonal complexes regarding infection evolution delay and comparison of their capacities to invade bone cells, induce cytotoxicity, and convert to a small-colony variant phenotype

		BJI chronicity					
CC	**Total**	**Acute BJI**	**Chronic BJI**	**Internalization rate**	**LDH release**	**SCV proportion**	**Delta-toxin negative**
CC5	18 (19%)	13 (20%)	5 (16%)	215% (136–294)	77% (69–86)	3% (2–4)	6 (33%)
CC30	17 (18%)	10 (16%)	7 (23%)	170% (106–234)	85% (77–92)	5% (3–6)	1 (6%)
CC45	12 (13%)	10 (16%)	2 (7%)	280% (81–479)	97% (73–121)	3% (2–4)	1 (8%)
CC15	10 (11%)	8 (13%)	2 (7%)	186% (90–282)	94% (71–117)	2% (1–3)	3 (30%)
CC398	9 (10%)	6 (9%)	3 (10%)	103% (71–135)	72% (58–87)	3% (2–4)	1 (11%)
CC8	8 (8%)	3 (5%)	5 (16%)	248% (111–386)	79% (58–100)	5% (2–8)	0 (0%)
CC25	6 (6)	4 (6%)	2 (7%)	171% (−17 to 358)	89% (49–129)	3% (1–5)	1 (17%)
Others	10 different CC with less than 5 isolates each						

Abbreviations: BJI, bone and joint infection; CC, Clonal complex; LDH, lactate dehydrogenase; SCV, small-colony variant.
Note: Results are presented as effective (%) and mean (95% CI) values and are expressed relative to the results obtained with the 8325-4 reference strain.

CI, 82.0–93.7), corresponding to 2.8% (95% CI, 0.6–5.0) versus 11.0% (95% CI, 8.9-13.0) of cell death; $p < 0.001$), and an accelerated biofilm formation at each measurement point (Fig. 4). No difference was detected regarding intracellular phenotype switching to SCV (2.5%; 95% CI, 1.7–3.1) for the delta-toxin-negative isolates versus 3.5% for the delta-toxin-positive isolates (95% CI, 3.0–3.9; p 0.153). Of note, the delta-toxin-negative isolates were not significantly associated with one of the seven major staphylococcal clonal complexes (p 0.181).

Discussion

Staphylococcal osteoblast invasion is considered as a patho-physiological pathway of BJI on the basis of *in vivo* observations

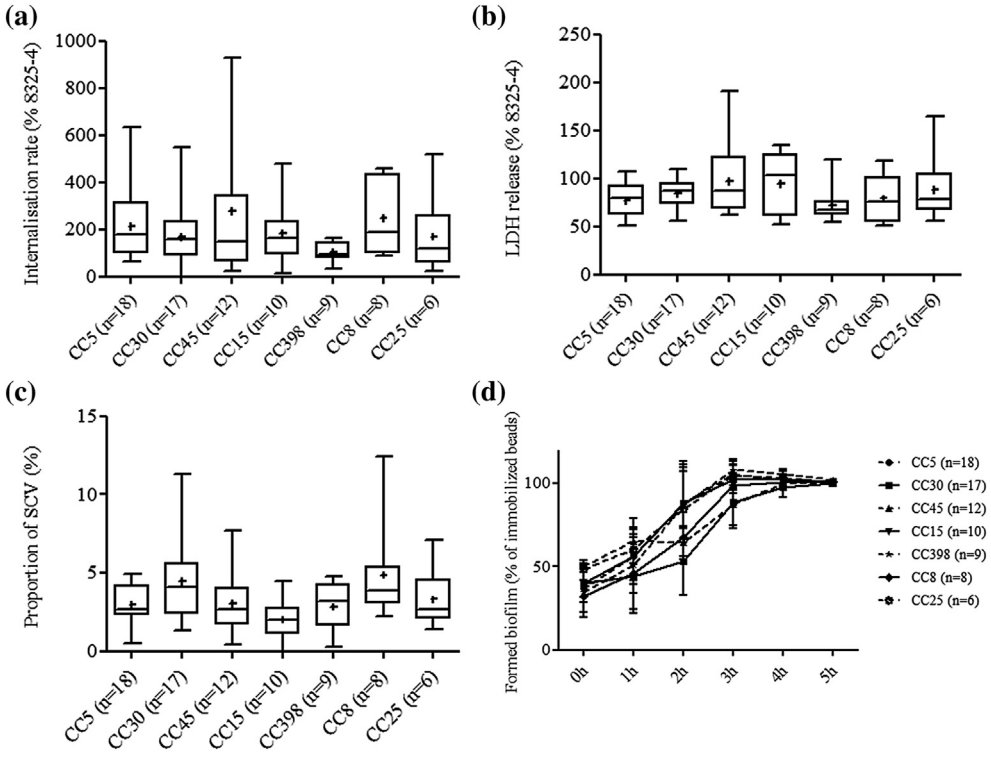

FIG. 3. Comparison of the major methicillin-susceptible Staphylococcus aureus (MSSA) bone and joint infection (BJI) clones regarding their capacities to invade bone cells, induce cytotoxicity, convert to a small-colony variant (SCV) phenotype, and form biofilm. (a) Internalization rate of MSSA isolates within human osteoblasts; (b) cytotoxicity rate induced by human osteoblast infection by MSSA isolates; (c) proportion of phenotype switching to SCVs; (d) biofilm formation.

TABLE 3. Distribution of virulence genes among acute and chronic bone and joint infection methicillin-susceptible *Staphylococcus aureus* isolates and determinants of infection chronicity

	Descriptive data				Univariate analysis		Multivariate analysis	
	Total	Acute BJI	Chronic BJI	p value	OR (95% CI)	p value	OR (95% CI)	p value
Sex (male)	60 (63%)	38 (59%)	22 (71%)	0.503	1.436 (0.582–3.546)	0.432		
Age (year)	53.6 (49.6–57.6)	56.1 (51.3–60.8)	48.5 (49.6–57.6)	0.105	0.984 (0.962–1.007)	0.175		
Modified Charlson score	2.6 (2.1–3.2)	2.9 (2.2–3.6)	2.0 (1.1–2.9)	0.148	0.881 (0.737–1.053)	0.164		
Internalization rate					1.000 (1.000–1.000)	0.101	1.000 (1.000–1.000)	0.244
LDH release					1.000 (1.000–1.000)	0.235		
SCV					1.000 (1.000–1.000)	0.875		
Delta-toxin negative					2.832 (0.920–8.715)	0.069	0.397 (0.708–8.112)	0.160
***agr* alleles**				0.561	0.896 (0.525–1.532)	0.689		
agr I	42 (44%)	26 (41%)	16 (52%)		1.559 (0.658–3.696)	0.313		
agr II	29 (31%)	22 (34%)	7 (23%)		0.557 (0.207–1.495)	0.245		
agr III	23 (24%)	15 (23%)	8 (26%)		1.136 (0.422–3.060)	0.801		
agr IV	1 (1%)	1 (2%)	0 (0%)		NC	NC		
Toxins								
tst	16 (17%)	11 (17%)	5 (16%)	1.000	0.927 (0.291–2.946)	0.897		
enterotoxins								
Sea	17 (18%)	12 (19%)	5 (16%)	1.000	0.833 (0.265–2.618)	0.755		
Seb	6 (6%)	4 (6%)	2 (7%)	1.000	1.034 (0.179–5.979)	0.970		
Sec	7 (7%)	7 (11%)	0 (0%)	0.092	NC	NC		
Sed	8 (9%)	6 (9%)	2 (7%)	1.000	0.690 (0.131–3.641)	0.662		
See	0 (0%)	0 (0%)	0 (0%)	NC	NC	NC		
Seg	58 (62%)	41 (65%)	17 (55%)	0.373	0.652 (0.271–1.566)	0.338		
She	10 (11%)	7 (11%)	3 (10%)	1.000	0.872 (0.210–3.632)	0.851		
Sei	59 (62%)	42 (66%)	17 (55%)	0.369	0.636 (0.265–1.527)	0.311		
Sej	7 (7%)	5 (8%)	2 (7%)	1.000	0.814 (0.149–4.450)	0.812		
Sek	5 (5%)	5 (8%)	0 (0%)	0.169	NC	NC		
seL	7 (7%)	7 (11%)	0 (0%)	0.092	NC	NC		
Sem	59 (62%)	42 (66%)	17 (55%)	0.369	0.636 (0.265–1.527)	0.311		
Sen	58 (61%)	41 (64%)	17 (55%)	0.501	0.681 (0.285–1.630)	0.388		
Seo	59 (62%)	42 (66%)	17 (55%)	0.369	0.636 (0.265–1.527)	0.311		
Seq	5 (5%)	5 (8%)	0 (0%)	0.169	NC	NC		
Ser	7 (7%)	5 (8%)	2 (7%)	1.000	0.814 (0.146–4.450)	0.812		
Seu	59 (62%)	42 (66%)	17 (55%)	0.369	0.636 (0.265–1.527)	0.311		
*luk*S-PV–*luk*F-PV (PVL)	0 (0%)	0 (0%)	0 (0%)	NC	NC	NC		
*luk*D–*luk*E	52 (55%)	34 (53%)	18 (58%)	0.668	1.222 (0.514–2.904)	0.650		
*luk*M–*luk*F-PV	0 (0%)	0 (0%)	0 (0%)	NC	NC	NC		
*luk*X	62 (90%)	41 (93%)	21 (84%)	0.245	0.384 (0.079–1.877)	0.237		
*luk*Y	65 (68%)	43 (67%)	22 (71%)	0.816	1.194 (0.469–3.040)	0.710		
Exfoliative toxins								
eta	0 (0%)	0 (0%)	0 (0%)	NC	NC	NC		
etb	0 (0%)	0 (0%)	0 (0%)	NC	NC	NC		
etd	6 (6%)	4 (6%)	2 (7%)	1.000	1.034 (0.179–5.979)	0.970		
HLB conv phages								
sak	72 (76%)	48 (75%)	24 (77%)	1.000	1.143 (0.414–3.152)	0.796		
chp	68 (72%)	48 (75%)	20 (65%)	0.336	0.606 (0.240–1.533)	0.290		
scn	90 (95%)	61 (95%)	29 (94%)	0.660	0.713 (0.113–4.504)	0.719		
Proteases								
*spl*A	52 (55%)	34 (53.1%)	18 (58.1%)	0.668	1.222 (0.514–2.904)	0.650		
*spl*B	52 (55%)	34 (53.1%)	18 (58.1%)	0.668	1.222 (0.514–2.904)	0.650		
*spl*E	48 (51%)	30 (46.9%)	18 (58.1%)	0.383	1.569 (0.660–3.731)	0.308		
Superantigens								
*set*C	65 (68%)	43 (67%)	22 (71%)	0.816	1.194 (0.469–3.040)	0.710		
*set*6	94 (99%)	64 (100%)	30 (97%)	0.326	NC	NC		
*ssl*1	95 (100%)	64 (100%)	31 (100%)	NC	NC	NC		
*ssl*2	95 (100%)	64 (100%)	31 (100%)	NC	NC	NC		
*ssl*3	69 (73%)	45 (70%)	24 (77%)	0.624	1.448 (0.534–3.928)	0.468		
*ssl*4	82 (94%)	55 (95%)	27 (93%)	1.000	0.736 (0.116–4.672)	0.745		
*ssl*5	95 (100%)	64 (100%)	31 (100%)	NC	NC	NC		
*ssl*6	23 (24%)	14 (22%)	9 (29%)	0.455	1.461 (0.551–3.877)	0.446		
*ssl*7	94 (99%)	63 (98%)	31 (100%)	1.000	NC	NC		
*ssl*8	54 (57%)	36 (56%)	18 (58%)	1.000	1.077 (0.452–2.564)	0.867		
*ssl*9	95 (100%)	64 (100%)	31 (100%)	NC	NC	NC		
*ssl*10	90 (100%)	61 (100%)	29 (100%)	NC	NC	NC		
*ssl*11	64 (70%)	43 (68%)	21 (72%)	0.809	1.221 (0.462–3.227)	0.687		
Capsule and biofilm-associated genes								
*cap*1	0 (0%)	0 (0%)	0 (0%)	NC	NC	NC		
*cap*5	45 (47%)	28 (44%)	17 (55%)	0.382	1.561 (0.659–3.699)	0.312		
*cap*8	50 (53%)	36 (56%)	14 (45%)	0.382	0.641 (0.270–1.518)	0.312		
*ica*A	95 (100%)	64 (100%)	31 (100%)	NC	NC	NC		
*ica*C	95 (100%)	64 (100%)	31 (100%)	NC	NC	NC		
*ica*D	95 (100%)	64 (100%)	31 (100%)	NC	NC	NC		
bap	1 (1%)	0 (0%)	1 (3%)	0.326	NC	NC		
Adhesins (MSCRAMMs)								
bbp	87 (92%)	59 (92%)	28 (90%)	0.713	0.791 (0.176–3.546)	0.791		
*clf*A	95 (100%)	64 (100%)	31 (100%)	NC	NC	NC		
*clf*B	95 (100%)	64 (100%)	31 (100%)	NC	NC	NC		
cna	41 (43%)	30 (47%)	11 (36%)	0.378	0.623 (0.257–1.510)	0.295		
ebh	93 (98%)	63 (98%)	30 (97%)	0.548	0.476 (0.029–7.876)	0.604		
*ebp*S	95 (100%)	64 (100%)	31 (100%)	NC	NC	NC		
eno	95 (100%)	64 (100%)	31 (100%)	NC	NC	NC		
fib	54 (57%)	36 (56%)	18 (58%)	1.000	1.077 (0.452–2.564)	0.867		
*fnb*A	95 (100%)	64 (100%)	31 (100%)	NC	NC	NC		
*fnb*B	84 (88%)	56 (88%)	28 (90%)	1.000	1.333 (0.328–5.419)	0.688		

TABLE 3. Continued

	Descriptive data				Univariate analysis		Multivariate analysis	
	Total	Acute BJI	Chronic BJI	p value	OR (95% CI)	p value	OR (95% CI)	p value
map	92 (99%)	61 (95%)	31 (100%)	0.548	NC	NC		
sasG	45 (47%)	30 (47%)	15 (48%)	1.000	1.062 (0.450–2.507)	0.890		
sdrC	94 (99%)	64 (100%)	30 (97%)	0.326	NC	NC		
sdrD	75 (79%)	54 (84%)	21 (68%)	0.105	0.389 (0.141–1.069)	0.067	0.365 (0.128–1.038)	0.059
vwb	95 (100%)	64 (100%)	31 (100%)	NC	NC	NC		
isaB	50 (56%)	33 (55%)	17 (59%)	0.822	1.159 (0.473–2.843)	0.747		
hsdS1	0 (0%)	0 (0%)	0 (0%)	NC	NC	NC		
hsdS2	73 (77%)	50 (78%)	23 (74%)	0.796	0.805 (0.296–2.186)	0.670		
hsdS3	60 (63%)	39 (61%)	21 (68%)	0.651	1.346 (0.545–3.328)	0.520		
hysA1	94 (99%)	64 (100%)	30 (97%)	0.326	NC	NC		
hysA2	86 (91%)	56 (88%)	30 (97%)	0.263	4.286 (0.512–35.906)	0.180		

Abbreviations: BJI, bone and joint infection; LDH, lactate dehydrogenase; NC: Not calculable; SCV, small-colony variant.
Note: Results are expressed as effective values (%). For each virulence factor, isolates with ambiguous detection were excluded from the denominator. For comparison between acute and chronic BJI, p-values were calculated for each gene or allele using a two-tailed Fisher exact test. Association with chronicity was assessed using a binary logistic regression analysis, including variables with p-values <0.15 in the final regression model.

and results obtained from *ex vivo* models of osteoblast infection, though using only a few reference *S. aureus* isolates [6–8]. Intracellular persistence may constitute a strategy to escape the action of the host immune system and antibiotics with exclusive extracellular diffusion, constituting a bacterial reservoir that can lead to chronicity or relapse [8]. This hypothesis has been previously investigated in our laboratory using the main circulating methicillin-resistant *S. aureus* (MRSA) clones, showing that community-acquired MRSA, usually responsible for acute forms of BJI, were more cytotoxic and less internalized in osteoblasts than hospital-acquired MRSA, known to more frequently induce indolent and recurrent BJI [16]. The present

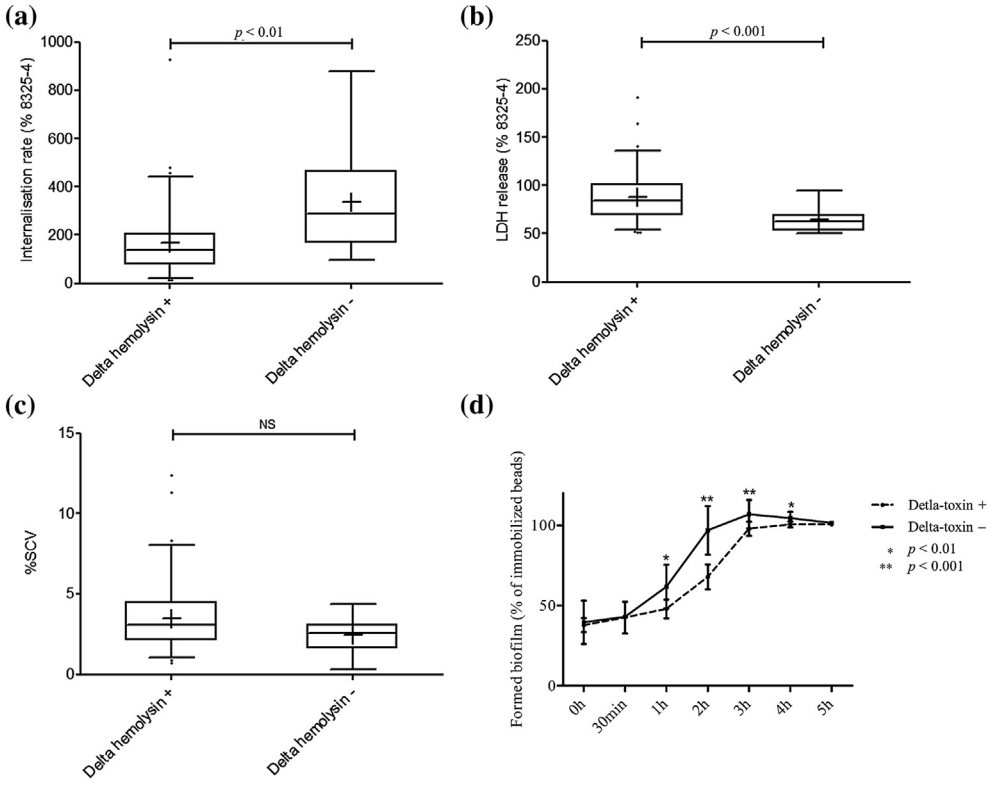

FIG. 4. Osteoblast invasion, cytotoxicity, and small-colony variant (SCV) intracellular emergence of methicillin-susceptible *Staphylococcus aureus* (MSSA) bone and joint infection (BJI) isolates regarding the bacterial production of delta-toxin. (a) Internalization rate of MSSA isolates within human osteoblasts; (b) cytotoxicity rate induced by human osteoblast infection with MSSA isolates; (c) proportion of phenotype switching to SCVs; (d) biofilm formation.

results confirm the association between the staphylococcal invasion of human osteoblasts and BJI chronicity for the first time among a large and highly diverse collection of clinical MSSA isolates. Conversely, this important diversity in bacterial genetic background may explain the difficulty in identifying any difference in cytotoxicity between chronic and acute BJI isolates, and the less clear differences better than studies using a few well-characterized laboratory reference isolates. Similarly, we failed to disclose any association between chronicity and the intracellular emergence of SCV. However, an accurate definition of SCV, involving not only colony sizes but also metabolism markers, for example, is lacking and may have helped to associate this phenotype with chronic BJI forms. Indeed, SCVs have been associated with *S. aureus* implanted-material infection and BJI recurrence [9,10], and cell invasion has been described as a putative mechanism of interconversion from the wild type to the SCV phenotype [11].

The high genetic diversity of our isolate collection, the absence of a direct relationship between BJI chronicity and bacterial genetic backgrounds or virulence factors, and the association of osteoblast invasion with *agr* deficiency all suggest that an intra-osteoblastic lifestyle is an adaptive staphylococcal mechanism leading to BJI chronicity rather than merely an intrinsic feature. Indeed, the comparison of *agr* expression at different time points during various infections has shown that acute infections are usually associated with a functional *agr* system [13]. The *agr* dysfunction appears to occur during the course of infection and in cases of persistent bacteraemia, diabetic foot infection or pulmonary infection in cystic fibrosis patients [12,13,23,26]. Additionally, chronicity of infection appeared to be the major factor associated with *agr* dysfunction in a previous series of 168 unselected clinical isolates [23].

In addition to the finding of a higher evolution delay of BJI in *agr*-deficient isolates, our results revealed a strong association between *agr* dysfunction and the bacterial phenotypic mechanisms associated with BJI chronicity, including: an enhanced biofilm formation, which had been previously suggested using various laboratory strains and a few clinical isolates from inhomogeneous pathological conditions [14,27,28]; and an increased osteoblastic invasion, with reduced infection-induced cytotoxicity. To our knowledge, the association of *agr* dysfunction and non-professional phagocytic cell invasion has only been described in airway epithelial cells [28]. Interestingly, using isogenic mutants, we also linked the intraosteoblastic cytotoxic phenotype of MRSA with the regulation of phenol-soluble modulins (PSMs), which can be considered as major effectors of intracellular staphylococcal virulence [16]. Indeed, once internalized, *S. aureus* is initially trapped in phagosomes [29]. PSM release may then results in phagosome membrane disruption, leading to translocation of PSM in the cytosol, and ultimately to host cell death [16]. Of note, PSM expression is under direct control of *agr* and delta-toxin is known itself as one of these PSM, called PSM**γ**. Put together, these considerations may explain the reduced cell lysis observed in our study in delta-toxin negative isolates, consequently promoting the constitution of an intracellular staphylococcal reservoir leading to chronicity.

Finally, it has been demonstrated that *agr* functionality can be easily assessed by delta-toxin production using whole-cell MALDI-TOF spectrum analysis [22,23]. As MALDI-TOF-MS is increasingly being used in routine laboratory practice for bacterial identification [23,30], it may provide in the same run reliable information with respect to *S. aureus agr* functionality at the time of BJI diagnosis, that is, when impaired, a predictive marker of chronic infection [23]. It may provide pivotal information for clinicians who currently lack objective criteria to characterize the chronicity state of BJI in patients, and directly impact their management. Notably, in the case of prosthetic joint infection, the current guidelines arbitrarily tolerate implant retention in cases of infection lasting for less than 3–4 weeks, considering that surgical debridement associated with combination therapy including anti-biofilm molecules, such as rifampin, will avoid the development of chronicity and increase the cure rate [3]. However, this decision is often very difficult in clinical practice, first, because the delay of 3–4 weeks is only theoretical, as bacterial adhesion and biofilm formation are highly likely to occur in the first hours of infection; and second, the clinical onset of infection is often difficult to determine because of the frequent occult evolution of BJI. In practice, these factors contribute to a failure rate of implant retention strategies that generally approaches 20% but can reach 50% in some poorly explained cases [2,31,32]. Hence, prospective evaluations of strategies using *agr*-deficiency detection at the time of diagnosis to help in the management of BJI as acute or chronic infections should be a priority according to their potential clinical impact.

Conclusions

Using a large and non-clonal clinical collection of BJI MSSA isolates, our findings suggest that bacterial invasion and intracellular life switching within bone cells constitute a pivotal pathophysiological mechanism of staphylococcal BJI chronicity, regardless of the genetic background of the isolate. Moreover, the loss of *agr* function that occurs during the infection course appears to be linked with BJI chronicity through the promotion of an intra-osteoblastic *S. aureus* reservoir by limiting intracellular staphylococcal cell damage and through the enhancement of biofilm formation. As a consequence, the detection of delta-toxin by

MALDI-TOF-MS, which is used in routine microbiology practice for bacterial identification, may provide a simple tool for the detection of isolates associated with chronic forms of BJI and may offer crucial help for clinical decisions in BJI management.

Funding

This work was supported by the French Ministry of Health, the French Ministry of Education, the Institut National de la Santé et de la Recherche Médicale (INSERM), the Groupement Inter-Regional à la Recherche Clinique et à l'Inovation (GIRCI-D50829 to J.P.R), and bioMérieux (to F. Vandenesch). The funders had no role in study design, data collection and analysis, the decision to publish, or manuscript preparation.

Transparency declaration

The authors declare that they have no conflicts of interest.

Acknowledgements

Lyon Bone and Joint Infection Study Group: Physicians—Tristan Ferry, Thomas Perpoint, André Boibieux, François Biron, Florence Ader, Julien Saison, Florent Valour, Fatiha Daoud, Johanna Lippman, Evelyne Braun, Marie-Paule Vallat, Patrick Miailhes, Christian Chidiac, Dominique Peyramond; **Surgeons**—Sébastien Lustig, Philippe Neyret, Olivier Reynaud, Caroline Debette, Anthony Viste, Jean-Baptiste Bérard, Frédéric Dalat, Olivier Cantin, Romain Desmarchelier, Michel-Henry Fessy, Cédric Barrey, Francesco Signorelli, Emmanuel Jouanneau, Timothée Jacquesson, Pierre Breton, Ali Mojallal, Fabien Boucher, Hristo Shipkov; **Microbiologists**—Frederic Laurent, François Vandenesch, Jean-Philippe Rasigade, Céline Dupieux; **Nuclear Medicine**—Isabelle Morelec, Marc Janier, Francesco Giammarile; **Pharmacokinetics/Pharmacodynamics specialists**—Michel Tod, Marie-Claude Gagnieu, Sylvain Goutelle; **Clinical Research Assistant**—Eugénie Mabrut.

References

[1] Lew DP, Waldvogel FA. Osteomyelitis. Lancet 2004;364:369–79.
[2] Zimmerli W, Trampuz A, Ochsner PE. Prosthetic-joint infections. N Engl J Med 2004;351:1645–54.
[3] Osmon DR, Berbari EF, Berendt AR, Lew D, Zimmerli W, Steckelberg JM, et al. Diagnosis and management of prosthetic joint infection: clinical practice guidelines by the Infectious Diseases Society of America. Clin Infect Dis 2013;56:e1–25.
[4] Sanchez Jr CJ, Mende K, Beckius ML, Akers KS, Romano DR, Wenke JC, et al. Biofilm formation by clinical isolates and the implications in chronic infections. BMC Infect Dis 2013;13:47.
[5] Brady RA, Leid JG, Calhoun JH, Costerton JW, Shirtliff ME. Osteomyelitis and the role of biofilms in chronic infection. FEMS Immunol Med Microbiol 2008;52:13–22.
[6] Bosse MJ, Gruber HE, Ramp WK. Internalization of bacteria by osteoblasts in a patient with recurrent, long-term osteomyelitis. A case report. J Bone Joint Surg Am 2005;87:1343–7.
[7] Jevon M, Guo C, Ma B, Mordan N, Nair SP, Harris M, et al. Mechanisms of internalization of *Staphylococcus aureus* by cultured human osteoblasts. Infect Immun 1999;67:2677–81.
[8] Ellington JK, Harris M, Webb L, Smith B, Smith T, Tan K, et al. Intracellular *Staphylococcus aureus*. A mechanism for the indolence of osteomyelitis. J Bone Joint Surg Br 2003;85:918–21.
[9] Proctor RA, von Eiff C, Kahl BC, Becker K, McNamara P, Herrmann M, et al. Small colony variants: a pathogenic form of bacteria that facilitates persistent and recurrent infections. Nat Rev Microbiol 2006;4:295–305.
[10] Sendi P, Rohrbach M, Graber P, Frei R, Ochsner PE, Zimmerli W. *Staphylococcus aureus* small colony variants in prosthetic joint infection. Clin Infect Dis 2006;43:961–7.
[11] Tuchscherr L, Medina E, Hussain M, Völker W, Heitmann V, Niemann S, et al. *Staphylococcus aureus* phenotype switching: an effective bacterial strategy to escape host immune response and establish a chronic infection. EMBO Mol Med 2011;3:129–41.
[12] Fowler Jr VG, Sakoulas G, McIntyre LM, Meka VG, Arbeit RD, Cabell CH, et al. Persistent bacteremia due to methicillin-resistant *Staphylococcus aureus* infection is associated with agr dysfunction and low-level in vitro resistance to thrombin-induced platelet microbicidal protein. J Infect Dis 2004;190:1140–9.
[13] Traber KE, Lee E, Benson S, Corrigan R, Cantera M, Shopsin B, et al. agr function in clinical *Staphylococcus aureus* isolates. Microbiology 2008;154:2265–74.
[14] Vuong C, Saenz HL, Gotz F, Otto M. Impact of the agr quorum-sensing system on adherence to polystyrene in *Staphylococcus aureus*. J Infect Dis 2000;182:1688–93.
[15] Trouillet S, Rasigade JP, Lhoste Y, Ferry T, Vandenesch F, Etienne J, et al. A novel flow cytometry-based assay for the quantification of *Staphylococcus aureus* adhesion to and invasion of eukaryotic cells. J Microbiol Meth 2011;86:145–9.
[16] Rasigade JP, Trouillet-Assant S, Ferry T, Diep BA, Sapin A, Lhoste Y, et al. PSMs of hypervirulent *Staphylococcus aureus* act as intracellular toxins that kill infected osteoblasts. PLoS One 2013;8:e63176.
[17] Valour F, Trouillet-Assant S, Rasigade JP, Lustig S, Chanard E, Meugnier H, et al. *Staphylococcus* epidermidis in orthopedic device infections: the role of bacterial internalization in human osteoblasts and biofilm formation. PLoS One 2013;8:e67240.
[18] Cai Z, Chattopadhyay N, Liu WJ, Chan C, Pignol JP, Reilly M. Optimized digital counting colonies of clonogenic assays using ImageJ software and customized macros: comparison with manual counting. Radiat Biol 2011;87:1135–46.
[19] Chavant P, Gaillard-Martinie B, Talon R, Hebraud M, Bernardi T. A new device for rapid evaluation of biofilm formation potential by bacteria. J Microbiol Methods 2007;68:605–12.
[20] Liesse Iyamba JM, Seil M, Devleeschouwer M, Takaisi Kikuni NB, Dehaye JP. Study of the formation of a biofilm by clinical strains of *Staphylococcus aureus*. Biofouling 2011;27:811–21.
[21] Novick RP, Geisinger E. Quorum sensing in staphylococci. Annu Rev Genet 2008;42:541–64.
[22] Janzon L, Lofdahl S, Arvidson S. Identification and nucleotide sequence of the delta-lysin gene, hld, adjacent to the accessory gene regulator (agr) of *Staphylococcus aureus*. Mol Gen Genet 1989;219:480–5.
[23] Gagnaire J, Dauwalder O, Boisset S, Khau D, Freydière AM, Ader F, et al. Detection of *Staphylococcus aureus* delta-toxin production by whole-cell MALDI-TOF mass spectrometry. PLoS One 2012;7:e40660.

[24] Bergeron M, Dauwalder O, Gouy M, Freydiere AM, Bes M, Meugnier H, et al. Species identification of staphylococci by amplification and sequencing of the tuf gene compared to the gap gene and by matrix-assisted laser desorption ionization time-of-flight mass spectrometry. Eur J Clin Microbiol Infect Dis 2011;30:343–54.

[25] Monecke S, Slickers P, Ehricht R. Assignment of *Staphylococcus aureus* isolates to clonal complexes based on microarray analysis and pattern recognition. FEMS Immunol Med Microbiol 2008;53:237–51.

[26] Park SY, Chong YP, Park HJ, Park KH, Moon SM, Jeong JY, et al. agr Dysfunction and persistent methicillin-resistant *Staphylococcus aureus* bacteremia in patients with removed eradicable foci. Infection 2013;41:111–9.

[27] Coelho LR, Souza RR, Ferreira FA, Guimaraes MA, Ferreira-Carvalho BT, Figueiredo AM. agr RNAIII divergently regulates glucose-induced biofilm formation in clinical isolates of *Staphylococcus aureus*. Microbiology 2008;154:3480–90.

[28] Ferreira FA, Souza RR, de Sousa Moraes B, de Amorim Ferreira AM, Américo MA, Fracalanzza SE, et al. Impact of agr dysfunction on virulence profiles and infections associated with a novel methicillin-resistant *Staphylococcus aureus* (MRSA) variant of the lineage ST1-SCCmec IV. BMC Microbiol 2013;13:93.

[29] Sinha B, Fraunholz M. *Staphylococcus aureus* host cell invasion and post-invasion events. Int J Med Microbiol 2010;300:170–5.

[30] Seng P, Drancourt M, Gouriet F, La Scola B, Fournier PE, Rolain JM, et al. Ongoing revolution in bacteriology: routine identification of bacteria by matrix-assisted laser desorption ionization time-of-flight mass spectrometry. Clin Infect Dis 2009;49:543–51.

[31] Marculescu CE, Berbari EF, Hanssen AD, Steckelberg JM, Harmsen SW, Mandrekar JN, et al. Outcome of prosthetic joint infections treated with debridement and retention of components. Clin Infect Dis 2006;42:471–8.

[32] Lora-Tamayo J, Murillo O, Iribarren JA, Soriano A, Sánchez-Somolinos M, Baraia-Etxaburu JM, et al. A large multicenter study of methicillin-susceptible and methicillin-resistant *Staphylococcus aureus* prosthetic joint infections managed with implant retention. Clin Infect Dis 2013;56:182–94.